Molecular Crystals and Liquid Crystals

Publication details, including instructions for authors and subscription information:
http://www.tandfonline.com/loi/gmcl20

Preparation and Characterization of Inclusion Compounds Using TEMPOL and an Organic 1-D Nanochannel as a Template

Hirokazu Kobayashi [a], Takahiro Ueda [a b], Keisuke Miyakubo [b], Taro Eguchi [a b] & Atsushi Tani [b]

[a] The Museum of Osaka University, Osaka University, Toyonaka, Osaka, Japan

[b] Graduate School of Science, Osaka University, Toyonaka, Osaka, Japan

Version of record first published: 03 Aug 2009

To cite this article: Hirokazu Kobayashi, Takahiro Ueda, Keisuke Miyakubo, Taro Eguchi & Atsushi Tani (2009): Preparation and Characterization of Inclusion Compounds Using TEMPOL and an Organic 1-D Nanochannel as a Template, Molecular Crystals and Liquid Crystals, 506:1, 150-167

To link to this article: http://dx.doi.org/10.1080/15421400902987545

Mol. Cryst. Liq. Cryst., Vol. 506, pp. 150–167, 2009

ISSN: 1542-1406 print/1563-5287 online
DOI: 10.1080/15421400902987545

Taylor & Francis
Taylor & Francis Group

Preparation and Characterization of Inclusion Compounds Using TEMPOL and an Organic 1-D Nanochannel as a Template

Hirokazu Kobayashi[1], Takahiro Ueda[1,2], Keisuke Miyakubo[2], Taro Eguchi[1,2], and Atsushi Tani[2]
[1]The Museum of Osaka University, Osaka University, Toyonaka, Osaka, Japan
[2]Graduate School of Science, Osaka University, Toyonaka, Osaka, Japan

Inclusion of 4-hydroxy-2,2,6,6-tetramethyl-1-piperidinyloxyl (TEMPOL) radical into an organic one-dimensional (1-D) nanochannels formed in guest-free tris (o-phenylenedioxy)cyclotriphosphazene (TPP) was attempted. The inclusion of TEMPOL molecules adsorbed into the TPP nanochannel and their molecular orientation and dynamics were confirmed by temperature-dependent election spin resonance (ESR) measurements. In the specimens prepared by co-precipitation, the existence of 1-D spin diffusion was suggested from the ESR line shape, but the diffusion was not as effective as in the case of the TPP and 2,2,6,6-tetramethyl-1-piperidinyloxy (TEMPO) inclusion compound reported in our previous article. These results imply a new methodology for the preparation of a new organic magnet using TPP as a template.

Keywords: 1-D molecular arrangement; ESR; molecular dynamics; molecular orientation; TEMPOL; TPP

INTRODUCTION

A pseudo-hexagonal organic one-dimensional (1-D) nanochannel exists in guest-free tris(*o*-phenylenedioxy)cyclotriphosphazene [TPP, Scheme 1(a)]. Its pore diameter is adjustable from 0.46 (for guest-free TPP) to 1 nm depending on the guest size. The TPP nanochannel has been of interest as it can accommodate various guest molecules [1–6]. The basic structure of the TPP nanochannel is based on the hexagonal

Address correspondence to Hirokazu Kobayashi, Graduate School of Science, Kyoto University, Kyoto 606-8502, Japan. E-mail: hirawk@kuchem.kyoto-u.ac.jp

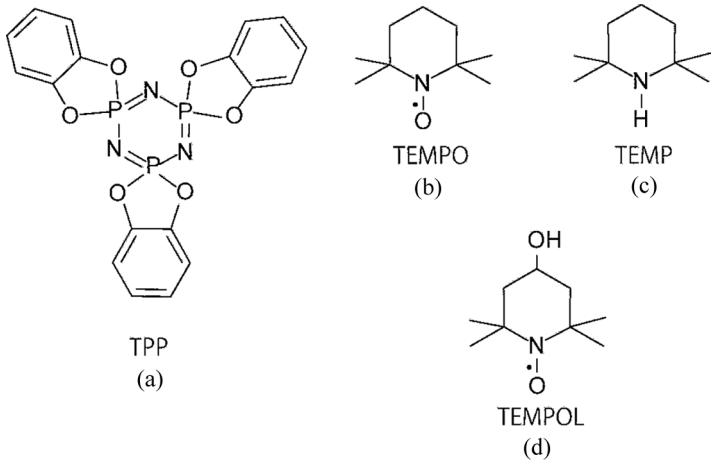

SCHEME 1 Chemical structures of the host and related guest compounds.

phase of TPP: its space group $P6_3/m$, $a = b = 1.1454$, $c = 1.016$ nm, $Z = 2$ [3]. The minimum framework of the TPP nanochannels (not the unit cell of the TPP hexagonal phase) is formed by three TPP molecules. Since the channel wall comprises phenyl rings of TPP molecules, in which the ring plane is parallel to the channel axis, the π electrons are rich on the channel surface. The channel surface homogeneity has been defined well using ^{129}Xe nuclear magnetic resonance (NMR) spectroscopy [7–9]. TPP nanochannels show a strong affinity for including simple-shaped gas molecules, and aliphatic or aromatic molecules [6,10–12]. The 1-D arrangement of functional molecules using the TPP nanochannel is particularly interesting from the point of view of developing new molecular devices, e.g., I_2 for anisotropic electron conductivity [13] and *p*-nitroaniline and its analogs for second harmonic generation [14,15].

Unfortunately, the construction of 1-D spin chains in the TPP nanochannels has been difficult because of the co-inclusion of solvent molecules [16]. Recently, we developed a new inclusion compound (IC) of 2,2,6,6-tetramethyl-1-piperidinyloxyl (TEMPO) [Scheme 1(b)] using TPP nanochannels as a template ($[TPP/TEMPO]_{IC}$), and confirmed the formation of 1-D molecular chains of TEMPO in TPP nanochannels [17]. Since $[TPP/TEMPO]_{IC}$ is constructed only from organic host and guest molecules, it is a candidate for a new organic magnet with a 1-D spin chain consisting of an unpaired electron localized on the 2p orbitals. The TPP crystal accommodates one TEMPO molecule per

two TPP molecules. The structure of TEMPO radicals in the TPP nanochannels could not be confirmed by single-crystal X-ray diffraction (XRD), even at 100 K. Instead, we obtained information about the molecular orientation of TEMPO in the TPP nanochannels by the spin probe technique using electron spin resonance (ESR) [18–21]. For the co-inclusion compound of TEMPO and 2,2,6,6-tetramethylpiperidine [TEMP, Scheme 1(c)], ($[TPP/(TEMPO)_{0.017} - (TEMP)_{0.983}]_{IC}$), it was shown that the TEMPO molecule undergoes uniaxial reorientation around the channel axis of TPP [22]. Detailed analyses of the powder patterns [23] revealed the orientation of the principle axes of **g** and hyperflne (**A**) tensors in TEMPO with respect to the channel axis, showing that the average direction of the N-O group of TEMPO is nearly perpendicular to the channel axis [24]. In addition, the temperature-dependent ESR spectra were characterized by the molecular motion of TEMPO depending on the temperature regions: the rigid-limit for $T < 128$ K; superposition of 60% uniaxial molecular rotation and 40% rigid components for $128\,K < T < 173$ K; and the uniaxial rotation of all TEMPO molecules for $T > 173$ K. It is reasonable to infer that the molecular orientation and dynamic behavior of TEMPO in $[TPP/TEMPO]_{IC}$ are approximated by those in $[TPP/(TEMPO)_{0.017}\text{-}(TEMP)_{0.983}]_{IC}$. These results can be related to temperature-dependent magnetism based on the following temperature ranges: paramagnetic interaction for $T < 139$ K; pure 1-D spin diffusion at $139\,K < T < 166$ K; and anisotropic 3-D antiferromagnetic interaction for $T > 166$ K [22].

For the design of a new organic magnet using TPP as a template, it is important to clarify the relationship between the inter-spin interaction and the molecular dynamics of guest molecules in the 1-D spin chain. The simplest way to control the rate of molecular rotational reorientation is to change the molecular size of the guest radicals because friction between the channel wall and the guest radicals increases concomitantly with increasing molecular size. Substitution of TEMPO with various functional groups enlarges the molecular size. Therefore, we attempted to prepare inclusion compounds using TPP and TEMPO derivatives.

In the present article, we chose 4-hydroxy-2,2,6,6-tetramethyl-1-piperidinyloxyl [TEMPOL, Scheme 1(d)] [25–30], one of the most popular TEMPO derivatives, as a guest compound for TPP. The preparation of the $[TPP/TEMPOL]_{IC}$ powder was attempted using the adsorption and co-precipitation methods, similar to the case of $[TPP/TEMPO]_{IC}$, and the resultant specimens were characterized by ESR, powder XRD and chemical analysis (CA). First, we will discuss the local structure of the included TEMPOL molecules in the TPP

nanochannels in the specimens prepared by vapor adsorption based on the temperature-dependent ESR spectra. Since most TPP nanochannels collapsed by heating in the adsorption method, only trace amounts of included TEMPOL were observed. On the other hand, in the co-precipitation method, the specimens co-including mesitylene as well as TPP and TEMPOL were prepared from a mixed mesitylene solution of TPP and TEMPOL. 1-D TEMPOL molecular arrangements and 1-D spin diffusion, which was weaker than in $[TPP/TEMPO]_{IC}$, were confirmed from the results of powder XRD and temperature-dependent ESR measurements. As a result, it was demonstrated that the co-precipitation method was more useful for including TEMPOL radical molecules into the TPP nanochannel. Eventually, we developed a new methodology for the preparation of $[TPP/TEMPOL]_{IC}$, in which no solvent molecule was co-included. These results shed new light on the design of a new organic magnet using TPP as a template.

EXPERIMENTAL METHOD

Chemicals

Tris(*o*-phenylenedioxy)cyclotriphosphazene (TPP) was synthesized as described in the literature [17]. The synthesized specimen was recrystallized twice from benzene for purification. A guest-free TPP powder specimen was prepared by heating at 348 K for three hours under reduced pressure. Both 1,3,5-trimethylbenzene (mesitylene) and 4-hydroxy-2,2,6,6-tetramethyl-1-piperidinyloxyl (TEMPOL) radical were purchased from Wako Pure Chemical Industries Ltd. and used without further purification.

Sample Preparation

The adsorption of TEMPOL molecules (m.p. 342–345 K) into the TPP nanochannels was carried out by exposure of TEMPOL vapor to guest-free TPP in an inverted Y-type test tube (12 mm o.d. and 10 mm i.d.) as follows. Guest-free TPP and TEMPOL were placed in each branch of the test tube at room temperature and the tube was sealed under reduced pressure ($P < 3 \times 10^{-2}$ kPa). The resultant ampoule was kept in an oven at 333 K for 6, 17, and 24 h for adsorption of the TEMPOL molecule. The starting colorless TPP powder was colored slightly pink during the initial adsorption time. At 343 K, TEMPOL was decomposed after more than 17 h adsorption. The specimens obtained using this procedure are denoted as compound **1**, and the treatment temperature and time are presented in parenthesis,

e.g., **1** (333 K, 6 h) for preparation by exposure of guest-free TPP to TEMPOL vapor at 333 K for 6 h.

The inclusion compound using TEMPOL and TPP using the co-precipitation method was prepared according to the following procedure. Powdered TPP (70–100 mg) and powdered TEMPOL (1.15 g) were dissolved in mesitylene (1 mL) at room temperature. The resultant solution was kept at ambient temperature for several hours at room temperature. Clear orange needle-shaped crystals were co-precipitated. All crystals were washed using water and then filtered. The specimens obtained using this procedure are denoted as compound **2**.

The resultant powder specimens prepared using the respective procedures were characterized using powder XRD. The adsorption amount of TEMPOL molecules was estimated using CA and spin concentration measurements were done using ESR. The desorption amount of TEMPOL from the inclusion compound was investigated using thermogravimetric analysis (TG). The desorption of TEMPOL was less than the adsorption amount evaluated by CA and ESR because of the low volatility of the guest compound (see below).

Powder XRD

Powder XRD analyses for all samples were carried out using a diffractometer (HP 9000 S712/60 Rotaflex Rint; Rigaku Corp.) with graphite monochromated Cu-Ka radiation ($\lambda = 0.154056$ nm) at room temperature. Data were collected in the θ–2θ scan mode using a 2θ scan rate of 2° min^{-1}; the 2θ collection range was 3–90°.

ESR Measurements

Powder ESR spectra were recorded using an X-band spectrometer (RE-IX; JEOL) at temperatures of 123 K to room temperature. Powdered specimens of 5–9 mg were packed in an ESR tube (270 mm long, o.d. 5 mmϕ) made from quartz glass, then capped using a teflon seal in a dried-air atmosphere. Thermal equilibrium of the sample was achieved by waiting 10–20 min after temperature changes. We also confirmed signal reproduction in both directions of increasing and decreasing temperature. The X-band microwave power was set to 0.01, 1, and 10 mW under non-saturated conditions. For g-factor determination, the magnetic field was measured accurately using a NMR detector (ES-FC5; JEOL) and a microwave counter (TR-5211A; Takeda Riken) with an experimental error of ± 0.001 mT. No line shape was distorted by excessive modulation amplitude based on a

plot of the square root of the microwave power versus the signal peak height. Spectral simulations of compound **1** and **2** were performed using the Chili program software package (EasySpin 2.7.1; ETH Zürich) [31,32].

RESULTS AND DISCUSSION

Chemical Analysis and Spin Concentration

Compositions of specimens prepared by the adsorption and co-precipitation methods were examined using CA and spin concentration measurements were obtained from the ESR signal intensities. Analysis of compound **1** (333 K, 6 h) revealed the following: H, 2.64%; C, 47.16%; N, 9.11%. Similar results were observed for compound **1** (333 K, 17 h) and **1** (333 K, 24 h) within experimental error. The results closely approximated the composition of guest-free TPP: H, 2.69%; C, 47.20%; N, 9.14%. The implication of these results is that only a trace amount of TEMPOL was accommodated in TPP. In contrast, the CA of the specimen prepared using the co-precipitation method (compound **2**) revealed H, 4.10%; C, 51.62%; N, 8.52%. This result demonstrates good agreement with the composition of a co-inclusion compound of TEMPOL and mesitylene (solvent) in TPP with the molar ratio of TPP:TEMPOL:mesitylene = 1:0.5:0.25 within experimental error (H, 4.20%; C, 51.66%; N, 8.52%).

The CA results are supported by spin concentration measurements. Compound 1 (333 K, 6 h) produced a very weak but detectable ESR signal (see below). The other two specimens, which were prepared using different times for TEMPOL adsorption, also yielded spectra with similar intensities and lines. The spin concentration was estimated as $2.2 \times 10^{19}\,g^{-1}$, which corresponds to 1/50 molar ratio to one TPP molecule. These facts suggest the inclusion of a trace amount of TEMPOL in the TPP nanochannels, or adsorption of a trace amount of TEMPOL on the surface of bulk TPP. Compound **2** gave an intense signal in the ESR spectrum. The signal intensity at room temperature (see below) indicated a spin concentration of $5.5 \times 10^{20}\,g^{-1}$. This concentration corresponds to the molar ratio of TPP:TEMPOL = 1:0.50 and is consistent with the expected value of $5.2 \times 10^{20}\,g^{-1}$ for the specimens with TPP:TEMPOL:mesitylene = 1:0.5:0.25 within experimental error.

The CA and spin concentration results suggest the preparation of a co-inclusion compound of TEMPOL and mesitylene with TPP by the co-precipitation method, but not by the adsorption method. Failure to form an inclusion compound of TEMPOL by the adsorption method could be attributed to the low volatility and small molecular size of

TEMPOL. The low volatility of TEMPOL lowers the vapor pressure being exposed to TPP, decreasing the possibility of accommodation of TEMPOL into the TPP nanochannels. Although heating is an easy way to increase the vapor pressure, decomposition of TEMPOL at temperatures greater than 343 K renders it difficult to obtain a sufficiently high vapor pressure to access the TPP nanochannel easily. Furthermore, the molecular size of TEMPOL (0.86 nm × 0.81 nm × 0.64 nm) [27] is too tight for its accommodation into the guest-free TPP nanochannel (0.46 nm minimum diameter), although the diameter of the TPP nanochannels depends on the guest molecule size. In the co-precipitation method, the co-existence of mesitylene as a solvent makes it possible to form the inclusion compound of TEMPOL with TPP. Mesitylene (0.90 nm × 0.86 nm × 0.40 nm) [33] has a similar molecular size to that of the TEMPOL molecule. It acts as a pillar of the channel structure for including large guest molecules. Compound **2**, prepared by the co-precipitation method, is stable to thermal treatment. The steric hindrance of the hydroxyl group of TEMPOL engenders low diffusivity of guest molecules, keeping them stable in the TPP nanochannel. However, these properties disturb precise TG. For example, the molar ratio of TEMPOL in compound **2** was estimated using TG as 0.3–0.4 per TPP molecule, which is an underestimation of the amount of guest molecules because of incomplete desorption.

Powder XRD for Inclusion Compound of TEMPOL with TPP

Figure 1 shows the powder XRD pattern of compound **1** (333 K, 6 h) [Fig. 1(a)] and those of some related substances [Figs. 1(b)–1(d)] at room temperature. The reflection of compound **1** (333 K, 6 h) was not coincident with the pseudo-hexagonal lattice of guest-free TPP, which is denoted by the red vertical bars in Fig. 1(d), but was similar to the monoclinic phase of TPP prepared by recrystallization from mesitylene solution, as presented in Fig. 1(b): $P2_1/n$, $a = 0.25086$ nm, $b = 0.5911$ nm, $c = 0.25913$ nm, $\beta = 95.97^\circ$ [4]. The peak positions estimated from these lattice parameters on the space group are marked by green vertical bars under Fig. 1(b). They are in good agreement with those of Fig. 1(a), especially in the low angle region ($2\theta < 13^\circ$). In fact, the pseudo-hexagonal lattice of guest-free TPP is known to change irreversibly to a monoclinic lattice by heating to temperatures higher than 373 K [4]. The monoclinic lattice does not form a channel or porous structure. Therefore, it cannot accommodate any guest compounds into its crystal lattice. The XRD result shows the collapse of the pseudo-hexagonal lattice of guest-free TPP by heating for a long time under reduced pressure in the preparation of compound **1**.

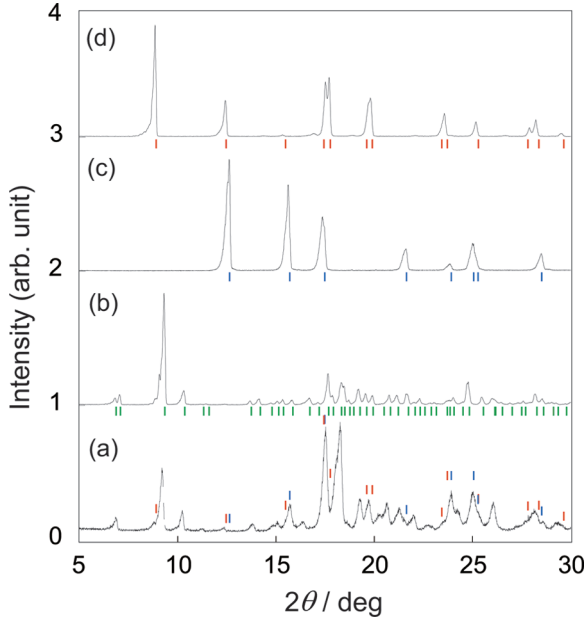

FIGURE 1 Powder XRD patterns of compound **1** (333 K, 6 h) (a) and various related compounds: TPP monoclinic phase recrystallized from mesitylene (b), bulk TEMPOL (c), and guest-free TPP nanochannel (d). Green, cyan and red vertical bars under (b), (c), and (d) are reflection patterns estimated by the lattice parameters and space group, respectively, described in previous reports [4], [36], and [6]. Cyan and red vertical bars in (a) show the corresponding peaks in (c) and (d).

However, a trace amount of reflection pattern corresponding to bulk TEMPOL and the pseudo-hexagonal lattice of guest-free TPP [Figs. 1(c) and 1(d)] was also observed in Fig. 1(a) (e.g., the peaks with $2\theta = 12.5$ and 15.8° in TEMPOL, and 8.9 and 19.8° in guest-free TPP). The corresponding peaks are represented as cyan and red vertical bars under Figs. 1(c) and 1(d), respectively, and the same colored vertical bars in Fig. 1(a). Consequently, these results show that compound **1** is composed of the following three components: monoclinic and pseudo-hexagonal (guest-free) TPP phases and the bulk TEMPOL phase. However, the fraction of pseudo-hexagonal phase is much less than the monoclinic phase, showing little accommodation of TEMPOL into the TPP nanochannel. Clearly, the adsorption method is unsuitable for preparation of the inclusion compound of TPP with TEMPOL.

Powder XRD reflection patterns of compound **2** at room temperature are depicted in Fig. 2 together with that of $[TPP/TEMPO]_{IC}$

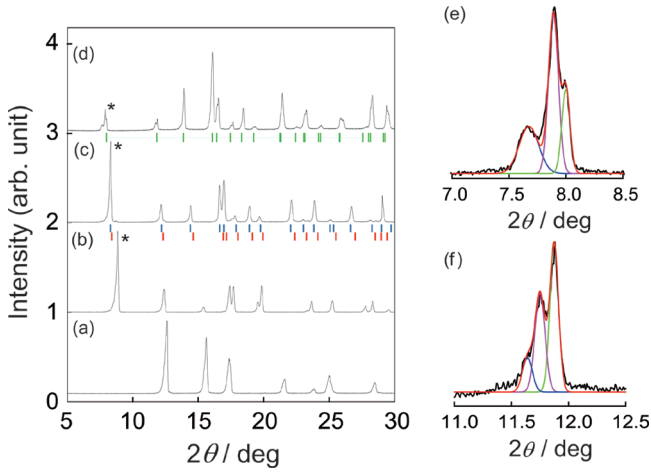

FIGURE 2 Powder XRD patterns of bulk TEMPOL (a), guest-free TPP (b), and $[TPP/TEMPO]_{IC}$ prepared by recrystallized method (c), and compound **2** (d). In (b)–(d), the reflection patterns are analogs of each other; the peaks are shifted to the lower degree side as the molecular cross-section of the guest compounds increases (e.g., see peaks marked by asterisks). Red vertical bars under (c) signify the reflection pattern estimated based on the pseudo-hexagonal TPP lattice of $[TPP/TEMPO]_{IC}$ at 100 K [17]. The cyan vertical bars show the estimates assuming expansion of the crystal at room temperature. The green vertical bars under (d) correspond to the reflection pattern estimated on the assumption that compound **2** belongs to the same space group of (c). Panels of (e) and (f) show enlarged views of (d) in the range of $2\theta = 7.0$–$8.5°$ and 11–12.5°. Both are reproducible by the superposition of three Gaussian functions.

prepared by the recrystallization method [17] and a few relevant materials. No reflections corresponding to bulk TEMPOL or guest-free TPP [Figs. 2(a) and 2(b)] were observed in compound **2** [Fig. 2(d)]. Figure 2(c) depicts reflection patterns of $[TPP/TEMPO]_{IC}$ prepared using recrystallization. Reflections in Figs. 2(b)–2(d) show similar patterns, but shift to the smaller angle side, suggesting enlargement of the lattice parameter, i.e., the diameter of the TPP nanochannels, by the inclusion of the guest compound. The larger the molecular cross section of the guest molecules, the lower the peak positions of the reflections [e.g., peaks marked by asterisks in Figs. 2(b)–2(d)]. For $[TPP/TEMPO]_{IC}$, the crystal structure of the TPP framework was determined using single-crystal XRD at 100 K. This crystal is classified in the monoclinic crystal system. The space group is $P2_1/m$ and the lattice parameters are $a = 1.2133$ nm, $b = 0.9830$ nm,

$c = 1.2147\,\text{nm}$, $\beta = 119.95^\circ$ [17]. The unit cell approximates a pseudo-hexagonal lattice because β is very close to 120°. The red vertical bars under Fig. 2(c) show reflections estimated using this lattice parameter. The observed reflections in Fig. 2(c) are slightly lower than the estimated ones, which indicate the expansion of the [TPP/TEMPO]$_{IC}$ crystal at room temperature. Assuming the same space group as the TPP pseudo-hexagonal lattice at 100 K, the lattice parameters can be evaluated as $a = c = 1.250\,\text{nm}$, $b = 0.990\,\text{nm}$. These lattice parameters yield the reflections represented as cyan vertical bars. The nanochannel diameter can be estimated using the interchannel distances of the guest-free TPP, i.e., the lattice parameter a ($a = b$ in hexagonal phase, and $a \sim c$ in the monoclinic phase).

Almost all peak positions in Fig. 2(d) correspond to Fig. 2(c), although the reflections shift to the lower angle side. The results implied that the TPP lattice of compound **2** might belong to the similar space group as [TPP/TEMPO]$_{IC}$. The lattice parameters of compound **2** were estimated as $a = 1.270\,\text{nm}$, $b = 1.015\,\text{nm}$, $c = 1.278\,\text{nm}$, $\beta = 119.95^\circ$. This result suggests that compound **2** has 1-D nanochannels and that the diameter expands in comparison with [TPP/TEMPO]$_{IC}$. The peak positions evaluated from these lattice parameters are depicted under Fig. 2(d) as green vertical bars.

However, the reflection patterns for 7.0–8.5° and 11–12.5 of 2θ in Fig. 2(d) seem to be superimposed by some components. Figures 2(e) and (f) show enlarged views of these peaks. These peaks are well reproduced by three Gaussian peaks, suggesting the existence of at least three components. These results suggest two possibilities about the composition of compound **2**: (1) mixtures of [TPP/TEMPOL]$_{IC}$, [TPP/mesitylene]$_{IC}$ and [TPP/(TEMPOL)$_x$-(mesitylene)$_y$]$_{IC}$ or (2) the degradation of the symmetry of the TPP lattice in a homogeneous crystal. Regarding (1), the lattice parameters in [TPP/mesitylene]$_{IC}$ (Table 1) give reflections at an angle larger than that for compound **2**. A reflection from the (100) plane in [TPP/mesitylene]$_{IC}$ is expected to be around 8.7° based on the space group and lattice parameter, which is inconsistent with the experimental results [2]. Therefore, possibility (2) is a more likely explanation of the composition of compound **2** than possibility (1).

According to results of the CA and spin concentration measurements, compound **2** includes TPP, TEMPOL, and mesitylene molecules with a molar ratio of TPP:TEMPOL:mesitylene = 4:2:1. Enlarging the lattice constant along the channel axis if compound **2** is monophase, the channel accommodates at least two TEMPOL and one mesitylene molecule. In this case, compound **2** will be represented as [TPP/(TEMPOL)$_{0.5}$-(mesitylene)$_{0.25}$]$_{IC}$.

Although the nanochannel of TPP is homogeneous, as revealed by ^{129}Xe NMR results [7–9], in fact, channel wall irregularities exist because of the repetition of the phenyl ring moiety. The bottleneck gives the minimum diameter, which corresponds to the diameter of a circle close to the plane of the phenyl rings. On the other hand, the maximum diameter corresponds to the interspace of the TPP layers. The inclusion of various guest molecules enlarges the channel diameters. The a values for some inclusion compounds of TPP are presented in Table 1 (the covalent radius of all molecules has been considered).

In an earlier study, we estimated a minimum diameter of the TPP nanochannels of $[TPP/TEMPO]_{IC}$ at 100 K to be 0.58 nm [22]. The TEMPO molecules are accommodated in the portion of the maximum diameter (0.85 nm) of the nanochannel in a molecular orientation in which the N-O bond is perpendicular to the channel axis. For compound **2**, the diameters are 0.63 nm for the minimum and 0.89 nm for the maximum part. The molecular cross-section of the TEMPOL molecule is about 20% greater than that of TEMPO because of the 4-hydroxyl group. In contrast, the minimum and maximum diameter of compound **2** is at most 7% larger than $[TPP/TEMPO]_{IC}$ at room temperature. This channel diameter expansion is sufficiently large to accommodate the TEMPOL molecule into the maximum diameter part in compound **2**. Furthermore, mesitylene is included in the TPP nanochannels of compound **2** as a guest molecule. According to ^{2}H NMR measurements, mesitylene molecules are lying on the

TABLE 1 Dependence of the interchannel distances of the TPP nanochannel on guest molecule size

Guest molecule	Space Group of TPP Lattice	Molecular size /nm^3	Interchannel distance (lattice parameter a)/nm
Free[*1]	$P6_3/m$	–	1.145
Benzene[*2]	$P6_3$ or $P6_3/m$	$0.57 \times 0.51 \times 0.34$	1.1804
o-xylene[*2]	$P6_3$ or $P6_3/m$	$0.72 \times 0.69 \times 0.40$	1.195
p-xylene[*2]	$P6_3$ or $P6_3/m$	$0.99 \times 0.51 \times 0.40$	1.168
mesitylene[*2]	$P6_3$ or $P6_3/m$	$0.90 \times 0.84 \times 0.40$	1.165
TEMPO at r.t. (calculated)	$P2_1/m$	$0.86 \times 0.67 \times 0.63$[*3]	1.250
TEMPOL and mesitylene (calculated)	$P2_1/m$	$0.88 \times 0.81 \times 0.64$ (TEMPOL)[*4]	1.270

[*1][6]; [*2][2]; [*3]In the monoclinic phase at a temperature of between 276 and 283 K [34]; [*4]In bulk crystal [27].

channel axis with an orientation in which the C_2 symmetry axis is parallel to the channel axis [35]. Assuming identical orientation to that of compound **2**, the estimated channel diameters can also accommodate mesitylene molecules in the TPP nanochannel. Further study of the structural details of compound **2** is now underway using single crystals.

ESR Study of the Local Structure of TEMPOL in TPP

Compound **1** yields a detectable ESR signal, although the inclusion of TEMPOL was not clearly confirmed using powder XRD. Figure 3 depicts the ESR spectrum in compound **1** (333 K, 6 h) at 223 K and room temperature. This spectrum was independent of temperature at less than 223 K.

The spectrum at 223 K [Fig. 3(a)] was well reproduced by the superposition of an isotropic Lorentzian peak with line width of $\Delta B_{pp} = 3.2$ mT (cyan line) and a resonance line of the isolated and rigid component (green line) as characterized by the **g** and **A** tensors with

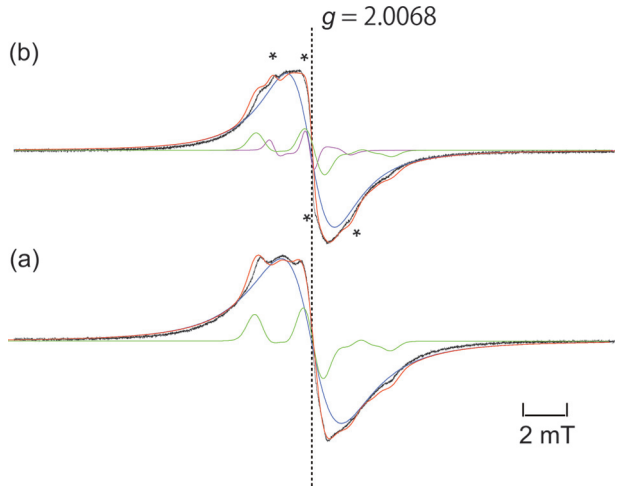

FIGURE 3 ESR spectra of compound **1** (333 K, 6 h) at 223 K (a) and room temperature (b). Spectrum (a) was reproduced by $(92 \pm 1)\%$ isotropic Lorentzian (cyan) and $(8 \pm 1)\%$ isolated and rigid-limit TEMPOL (green). In (b), the spin amount of the isotropic Lorentzian component was invariant, but the isolated TEMPOL component was split into two components with the population of $(7 \pm 0.5)\%$ (green) and $(1 \pm 0.5)\%$ (purple), respectively (marked by asterisks). The newly observed component is assigned to TEMPOL undergoing uniaxial reorientation.

$g_{xx} = 2.0099$, $g_{yy} = 2.0062$, $g_{zz} = 2.0024$, and $A_{xx} = 0.53$ mT, $A_{yy} = 0.75$ mT, and $A_{zz} = 3.35$ mT. The populations of the respective compounds were $(92 \pm 1)\%$ for the former and $(8 \pm 1)\%$ for the latter.

Figure 3(b) shows that this spectrum depends to some degree on temperature. A new component appeared corresponding to the isolated and rigid nitroxide radical. The new peaks are marked with asterisks in Fig. 3(b). The resultant spectrum is reproducible by the superposition of a triplet peak derived by the axial reorientation of TEMPOL molecules [purple line in Fig. 3(b)] in addition to the former two components, although the peak-to-peak line width (ΔB_{pp}) of a Lorentzian becomes narrower ($\Delta B_{pp} = 2.4$ mT). The population of each component was $(7 \pm 0.5)\%$ for a rigid TEMPOL and $(1 \pm 0.5)\%$ for a mobile one. It is noteworthy that the isotropic component population is independent of temperature.

For the isotropic component, two possibilities exist for the origin: (1) the concentrated TEMPOL molecules on the surface of bulk TPP and (2) a trace amount of TPP nanochannels. The bulk crystal of TEMPOL gives an isotropic Lorentzian resonance line with $\Delta B_{pp} = 0.7$ mT at room temperature, which is narrowed by exchange interaction between the spins on TEMPOL molecules [29]. In the former case, if the TEMPOL molecules on the surface of compound **1** are condensed with similar intermolecular interactions between the TEMPOL molecules as that in the bulk one, it is expected to yield a similar spectrum as the bulk crystal of TEMPOL. However, compound **1** gave a much broader resonance line than that of the bulk one, implying less effective exchange narrowing in compound **1**. Anisotropic space on the surfaces of microcrystal line compound **1** renders it difficult to grow TEMPOL bulk crystals. The imperfection of the molecular stacking probably engenders less effective exchange interaction, causing broadening of the line width of the isotropic component.

In the latter case, 1-D arrangement of TEMPOL molecules in the TPP nanochannels will enlarge the intermolecular distance of the neighboring TEMPOL molecules by the steric hindrance between the two bulky methyl groups. This situation will probably decrease the exchange interactions between the TEMPOL molecules, and cause line broadening by the dipolar interaction between spins. Consequently, these two simulations seem to be consistent with the experimental ESR spectrum at 223 K. This component also shows slight narrowing ($\Delta B_{pp} = 2.4$ mT) on heating, which should be modulated by molecular motion. However, the population of this component is independent of temperature, implying lower mobility of TEMPOL molecules in the concentrated region. Therefore, the isotopic part will be assigned as (1) and/or (2). Further analyses are now underway.

Regarding minor components, the **g** and **A** tensor components were consistent with those in the diluted TEMPOL trapped in a matrix of 4-hydroxy-2,2,6,6-tetramethyl-piperidine-1-oxyl (TEMP-OH) within experimental errors[28]: $g_{xx} = 2.0099$, $g_{yy} = 2.0061$, and $g_{zz} = 2.0024$; $A_{xx} = 0.53$ mT, $A_{yy} = 0.70$ mT, and $A_{zz} = 3.50$ mT. This result suggests that about 8% of TEMPOL molecules existed as isolated TEMPOL molecules. In this case, two TEMPOL molecules are for the isolated species: one is in the isolated void in the monoclinic TPP phase; the other is an inclusion into a trace amount of the guest-free TPP. The former will be independent of temperature because of tight accommodation in the interstitials of the bulk crystals.

In contrast, in the latter, the confined TEMPOL will undergo uniaxial molecular reorientation. Uniaxial reorientation of TEMPOL will give rise to a triplet peak broadened by axial symmetric **g** and **A** tensors, similar to TEMPO in $[TPP/TEMPO]_{IC}$ [24]. Assuming that the TEMPOL molecules have similar orientation to that of TEMPO in $[TPP/TEMPO]_{IC}$, and assuming that uniaxial reorientation of TEMPOL molecules takes place around the principle y axis approximately lying on the channel axis, the **g** and **A** tensors for the rigid component in Fig. 3(a) are partially averaged out to be $A_{\perp} = 3.87 \pm 0.03$ mT, $A_{\parallel} = 0.75 \pm 0.03$ mT, $g_{\perp} = 2.0062 \pm 0.0001$, and $g_{\parallel} = 2.0063 \pm 0.0001$, respectively, when the correlation time, τ_R, for molecular reorientation is 5×10^{-7} s. These averaged **g** and **A** tensors well reproduce the observed spectrum at room temperature, as depicted in Fig. 3(b). Similar temperature dependence of the ESR spectrum was also observed in compound **1** (333 K, 17 h) and **1** (333 K, 24 h).

Eventually, for the preparation of $[TPP/TEMPOL]_{IC}$ by the adsorption method, a milder experimental condition than this study is needed, e.g., long-time adsorption at lower temperature for preventing the collapse of the TPP nanochannels. In fact, to prepare homogeneous ICs, and to investigate the molecular motion and orientation of TEMPOL in the TPP nanochannels more precisely, a new specimen should be prepared by the co-precipitation method, such as a $[TPP/(TEMPOL)_x\text{-}(TEMP\text{-}OH)_y]_{IC}$, analogous to our previous study in $[TPP/(TEMPO)_x\text{-}(TEMP)_y]_{IC}$ [22,24]. Further works are now underway.

In compound **2**, the CA and the spin concentration measurements revealed the composition of $[TPP/(TEMPOL)_{0.5}\text{-}(mesitylene)_{0.25}]_{IC}$. Figure 4(a) depicts the temperature dependence of the ESR spectrum of compound **2**. The TEMPOL in compound **2** gives rise to a single isotropic resonance line at temperatures from 123 K to room temperature. The line width was much broader than that in the bulk TEMPOL ($\Delta B_{pp} = 0.7$ mT) and was somewhat narrowed with increasing

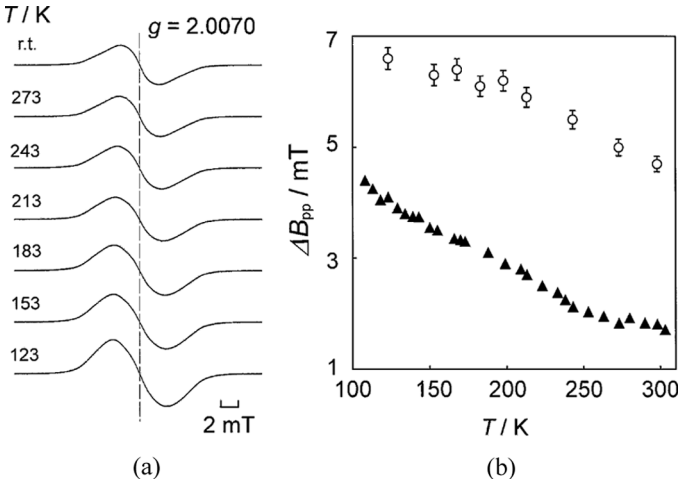

FIGURE 4 Temperature dependence of the ESR spectra in compound **2** (a) and line width (b). The line width of compound **2** was denoted as an open circle (o); that of $[TPP/TEMPO]_{IC}$ was denoted as filled triangles (▲). Data of line width in $[TPP/TEMPO]_{IC}$ are from our previous article [22].

temperature. As described above, the broad line width suggests a different environment of TEMPOL from that of the bulk one and it is conceivable that the TEMPOL molecules were accommodated in the TPP nanochannel.

The resonance line was well reproduced using a Gaussian of less than 213 K, although, at greater than 213 K, the contribution of Lorentzian was increased slightly. According to Dietz *et al*., the ESR line shape is affected by interspin interactions and the dimensionality of spin diffusion [36]. A pure Gaussian line shape is broadened by dipolar interaction. A pure Lorentzian line shape is narrowed by molecular motion or 3-D exchange interaction. An intermediate between Gaussian and Lorentizan for the line shape is narrowed by 1-D spin diffusion. The line shape of compound **2** at temperatures greater than 213 K shows that 1-D spin diffusion narrows the resonance line.

The temperature dependence of the peak-to-peak line width *(ΔB_{PP})* of the ESR spectrum in compound **2** is shown in Fig. 4(b) together with previous results from $[TPP/TEMPO]_{IC}$ [22]. The line width decreases slightly with increasing temperature. The ΔB_{pp} values in compound **2** are 1.5 times larger at 123 K, and 2.9 times larger at room temperature than those in $[TPP/TEMPO]_{IC}$. The line width of $[TPP/TEMPO]_{IC}$ is narrowed mainly by 1-D spin diffusion. Therefore, Fig. 4(b) exhibits a small degree of narrowing in compound **2** in

comparison with $[TPP/TEMPO]_{IC}$. That is, it is presumed that the line width in compound **2** is dominated mainly by magnetic dipolar interaction because of less effective exchange narrowing. For radicals in the TPP nanochannels, the through-space interaction is most preferable for the main mechanism for spin exchange. In compound **2,** mesitylene molecules co-included in TPP might act as a spacer, enlarging the interspin distance between the neighboring TEMPOL molecules.

CONCLUSION

Preparation of an IC using TEMPOL and TPP nanochannels as a template was attempted. The adsorption method was not very effective in preparing inclusion compounds. Temperature-dependent ESR spectra of the specimen prepared using the adsorption method (compound **1**) were reproduced using two components at 123 K, but three components at room temperature. Although compound **1** includes the monoclinic phase of TPP as a major component, a trace amount of TEMPOL was found which differs from the bulk one, indicating either adsorption on the surface of the TPP polycrystals or inclusion in the TPP nanochannel. Molecular orientation and dynamics of TEMPOL were analyzed according to the ESR spectrum. The principle *y* axis is parallel to the channel axis and undergoes uniaxial rotation around the axis similar to TEMPO in the TPP nanochannels, suggesting the inclusion of TEMPOL into the TPP nanochannel. Compound **2** was prepared using co-precipitation, and the resultant specimen was assigned as $[TPP/(TEMPOL)_{0.5}\text{-}(mesitylene)_{0.25}]_{IC}$. Powder XRD revealed that compound **2** maintains a pseudo-hexagonal structure of the TPP nanochannels. Enlargement of the lattice parameter supports the inclusion of TEMPOL and mesitylene into the TPP nanochannel. Furthermore, the ESR line shape in compound **2** suggests the existence of 1-D spin diffusion, but it is not as effective as in the case of $[TPP/TEMPO]_{IC}$. Co-inclusion of mesitylene, which serves as a spacer to enlarge the intermolecular distance between TEMPOL, probably weakens the exchange interaction between the spins on TEMPOL.

Therefore, we propose a new methodology for the preparation of $[TPP/TEMPOL]_{IC}$ and investigate its precise molecular orientation and dynamics. To prevent co-inclusion of solvent, other solvents with larger molecular size than that of TEMPOL should be used to prepare $[TPP/TEMPOL]_{1C}$. For instance, 1,3,5-triethylbenzene [3] is a suitable candidate for use as such a solvent. Many TEMPO derivatives have a similar cross section with TEMPOL. Therefore, these solvent molecules are also expected to be available for their preparation. Such ideas will be applicable to the design of a new organic magnet using

TPP as template. Further attempts for preparation and characterization of new inclusion compounds (ICs) using various organic radicals are now underway to investigate the relationship between molecular orientation, the dynamics of guest radicals, and spin–spin interactions.

REFERENCES

[1] Allcock, H. R. (1964). *J. Am. Chem. Soc*, *86*, 2591.
[2] Allcock, H. R., & Siegel, L. A. (1964). *J. Am. Chem. Soc.*, *86*, 5140.
[3] Allcock, H. R., Allen, R. W., Bisse, E. C., Smeltz, L. A., & Teeter, M. (1976). *J. Am. Chem. Soc.*, *98*, 5120.
[4] Allcock, H. R., Levin, M. L., & Whittle, R. R. (1986). *Inorg. Chem.*, *25*, 41.
[5] Sozzani, P., Comotti, A., Bracco, S., & Simonutti, R. (2004). *Angew. Chem. Int. Ed.*, *43*, 2792.
[6] Sozzani, P., Bracco, S., Comotti, A., Ferretti, L., & Simonutti, R. (2005). *Angew. Chem. Int. Ed.*, *44*, 1816.
[7] Meersmann, T., Logan, J. W., Simonutti, R., Caldarelli, S., Comotti, A., Sozzani, P., Kaiser, L. G., & Pines, A. (2000). *J. Phys. Chem. A*, *104*, 11665.
[8] Sozzani, P., Comotti, A., Simonutti, R., Meersmann, T., Logan, J. W., & Pines, A. (2000). *Angew. Chem. Int. Ed*, *39*, 2695.
[9] Kobayashi, H., Ueda, T., Miyakubo, K., & Eguchi, T. (2003). *Z. Naturforsch.*, *58a*, 727.
[10] Gahungu, G., Zhang, B., & Zhang, J. (2007). *J. Phys. Chem. B*, *111*, 5031.
[11] Couderc, G., Hertzsch, T., Behrnd, N.-R., Krämer, K., & Hulliger, J. (2006). *Micropor. Mesopor. Mater.*, *88*, 170.
[12] Sozzani, P., Comotti, A., Bracco, S., & Simonutti, R. (2004). *Chem. Comrnun.*, 768.
[13] Hertzsch, T., Budde, F., Weber, E., & Hulliger, J. (2002). *Angew. Chem. Int. Ed.*, *41*, 2281.
[14] Gervais, C., Hertzsch, T., & Hulliger, J. (2005). *J. Phys. Chem. B*, *109*, 7961.
[15] Hertzsh, T., Kluge, S., Weber, E., Budde, F., & Hulliger, J. (2001). *Adv. Mater.*, *13*, 1864.
[16] Süss, H. I., Wuest, T., Sieber, A., Althaus, R., Budde, F., Lüthi, H.-P., McManus, G. D., Rawson, J., & Hulliger, J. (2002). *Cryst. Eng. Comm.*, *4*, 432.
[17] Kobayashi, H., Ueda, T., Miyakubo, K., Toyoda, J., Eguchi, T., & Tani, A. (2005). *J. Mater. Chem.*, *15*, 872.
[18] Schindler, H., & Seelig, J. (1974). *J. Chem. Phys.*, *61*, 2946.
[19] Noda, Y., Shimono, S., Baba, M., Yamauchi, J., Ikuma, N., & Tamura, R. (2006). *J. Phys. Chem. B*, *110*, 23683.
[20] Garcia-Rubio, I., Braun, M., Gromov, I., Thöny-Meyer, L., & Schweiger, A. (2007). *Biophys. J.*, *82*, 1361.
[21] Libertini, L. J., Waggoner, A. S., Jost, P. C., & Griffith, O. H. (1969). *Proc. Natl. Acad. Sc. U.S. A.*, *64*, 13.
[22] Kobayashi, H., Ueda, T., Miyakubo, K., Eguchi, T., & Tani, A. (2007). *Bull. Chem. Soc. Jpn.*, *80*, 711.
[23] Freed, J. H., & Seelig, J. (1976). Spin labeling, theory and applications. In: *Spin Labeling, Theory and Applications*, Berliner, L. J. (Ed.), Chapter 3 and 10, Academic Press Inc: New York, p. 53, 373.
[24] Kobayashi, H., Ueda, T., Miyakubo, K., Eguchi, T., & Tani, A. (2008). *Phys. Chem. Chem. Phys.*, *9*, 1263.

[25] Lajzerowicz-Bonneteau, J. (1976). Spin labeling, theory and applications. In: *Spin Labeling, Theory and Applications*, Berliner, L. J. (Ed.), Chapter 6, Academic Press Inc: New York, p. 239.
[26] Lajzérowicz-Bonneteau, P. J. (1968). *Acta. Cryst. B*, *24*, 196.
[27] Berliner, L. J. (1970). *Acta. Cryst. B*, *26*, 1198.
[28] Tabak, M., Alonso, A., & Nascimento, O. R. (1983). *J. Chem. Phys.*, *79*, 1176.
[29] Yamauchi, J. (1971). *Bull. Chem. Soc. Jpn.*, *44*, 2301.
[30] Krelick, R. W. (1967). *J, Chem. Phys.*, *46*, 4260.
[31] Stoll, S., & Schweiger, A. (2006). *J. Magn. Reson.*, *178*, 42.
[32] Stoll, S., & Schweiger, A. (2007). *Biol Magn. Reson.*, *27*, 299.
[33] Capper, G., Davies, D. L., Fawcett, J., & Russell, D. R., (1995). *Acta Cryst. C.*, *51*, 578.
[34] Capiomont, A., & Lajzérowicz-Bonneteau, J. (1974). *Acta Cryst. B*, *30*, 2160.
[35] Meirovitch, E. (1984). *J. Phys. Chem.*, *88*, 6411.
[36] Dietz, R. E., Merritt, F. R., Dingle, R., Hone, D., Silbernagel, B. G., & Richards, P. M. (1971). *Phys. Rev. Lett.*, *26*, 1186.